A note on a swirling squirmer in a shear-thinning fluid ⓕ

Ⓘ H. Nganguia, Ⓘ K. Zheng, Ⓘ Y. Chen, Ⓘ O. S. Pak, and Ⓘ L. Zhu

COLLECTIONS

Note: This paper is part of the Special Topic, Invited Contributions from Early Career Researchers 2020.

ⓕ This paper was selected as Featured

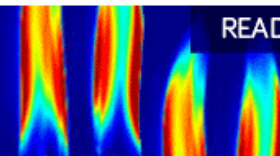# A note on a swirling squirmer in a shear-thinning fluid Ⓕ

View Online　　Export Citation　　CrossMark

H. Nganguia,[1] ⓘD K. Zheng,[2] ⓘD Y. Chen,[2] ⓘD O. S. Pak,[2,a)] ⓘD and L. Zhu[3,b)] ⓘD

AFFILIATIONS

[1] Department of Mathematical and Computer Sciences, Indiana University of Pennsylvania, Indiana, Pennsylvania 15705, USA
[2] Department of Mechanical Engineering, Santa Clara University, Santa Clara, California 95053, USA
[3] Department of Mechanical Engineering, National University of Singapore, 117575, Singapore

Note: This paper is part of the Special Topic, Invited Contributions from Early Career Researchers 2020.
[a)] Electronic mail: opak@scu.edu
[b)] Author to whom correspondence should be addressed: lailai_zhu@nus.edu.sg

ABSTRACT

Micro-organisms and artificial microswimmers often move in biological fluids displaying complex rheological behaviors, including viscoelasticity and shear-thinning viscosity. A comprehensive understanding of the effectiveness of different swimming gaits in various types of complex fluids remains elusive. The squirmer model has been commonly used to represent different types of swimmers and probe the effects of different types of complex rheology on locomotion. While many studies focused only on squirmers with surface velocities in the polar direction, a recent study has revealed that a squirmer with swirling motion can swim faster in a viscoelastic fluid than in Newtonian fluids [Binagia *et al.*, J. Fluid Mech. **900**, A4, (2020)]. Here, we consider a similar setup but focus on the sole effect due to shear-thinning viscosity. We use asymptotic analysis and numerical simulations to examine how the swirling flow affects the swimming performance of a squirmer in a shear-thinning but inelastic fluid described by the Carreau constitutive equation. Our results show that the swirling flow can either increase or decrease the speed of the squirmer depending on the Carreau number. In contrast to swimming in a viscoelastic fluid, the speed of a swirling squirmer in a shear-thinning fluid does not go beyond the Newtonian value in a wide range of parameters considered. We also elucidate how the coupling of the azimuthal flow with shear-thinning viscosity can produce the rotational motion of a swirling pusher or puller.

Published under license by AIP Publishing. https://doi.org/10.1063/5.0029068

I. INTRODUCTION

Locomotion at a low Reynolds number has garnered significant interdisciplinary interest, which is closely related to understanding cell motility,[1–3] designing active colloids for soft matter research,[4–6] or artificial microswimmers for biomedical applications.[7–9] Although earlier studies commonly assumed the surrounding fluid medium to be Newtonian, many biological fluids such as blood and mucus display complex rheological behaviors, including viscoelasticity and shear-thinning viscosity. A key question emerging from the recent literature is how these non-Newtonian rheological behaviors affect the locomotion of micro-organisms.[10,11] A better understanding will also inform the design of artificial microswimmers for operations in more realistic, complex biological environments.[12] While substantial efforts focused on swimming in a

viscoelastic fluid,[13–26] recent efforts have also begun to examine the effect of shear-thinning viscosity.[27–34] However, a complete knowledge of what types of swimmers and locomotory gaits can enhance or hinder propulsion in the presence of different non-Newtonian fluid behaviors remains elusive.

Among different types of swimmer models, the squirmer model has gained popularity for both its simplicity and biological relevance.[35] Lighthill and Blake first considered the swimming motion of a squirmer,[36,37] which consists of a spherical body with prescribed surface velocities, as a model for ciliary propulsion of micro-organisms such as *Paramecium* and *Volvox*.[38–40] The body of these ciliates is covered by many hair-like organelles called cilia, which beat in coordinated manners to propel the body. The beating motion of these cilia is represented by surface velocities on the squirmer surface. In addition, the squirmer model has been employed as a generic

locomotion model for different types of swimmers (e.g., pushers and pullers), by adjusting the distribution of surface velocities. The squirmer model has also been used to examine how different types of non-Newtonian rheology affect locomotion.[18,19,27,30,41–46] While a small speed enhancement was predicted to occur for pushers at small Deborah numbers,[43] fluid elasticity was shown to generally reduce the swimming speed of pushers, pullers, and neutral squirmers at larger Deborah numbers.[18,19] Similarly, pushers, pullers, and neutral squirmers were shown to swim slower in a shear-thinning fluid than in a Newtonian fluid.[27,30] However, it is also possible for shear-thinning rheology to enhance swimming when a higher squirming mode is included in the surface velocity distribution.[30,47]

Most studies on the squirmer model considered only radial and tangential surface velocities without including the azimuthal components until recently.[35] In addition to general analyses of azimuthal motion in Stokes flow,[48–50] Pedley *et al.* demonstrated the importance of including azimuthal swirl in the squirmer model in describing the dynamics observed in experiments with *Volvox*.[51] More recently, Binagia *et al.* considered a swirling squirmer in viscoelastic fluids described by the Giesekus and FENE-P models.[52] Specifically, an azimuthal mode corresponding to a rotlet dipole in Stokes flow was included in their analysis to represent the effect due to a rotating flagellum and counter-rotating body of a swimming micro-organism. Such a swirling squirmer was shown to exhibit marked speed enhancement, allowing it to swim faster than in a Newtonian fluid. Furthermore, the results based on varying Giesekus mobility (and hence varying the degree of shear-thinning) suggested that the shear-thinning effect would only diminish the enhancement. Therefore, it was concluded that the marked speed enhancement should be largely attributed to the coupling of fluid elasticity with the swirling flow.

In this paper, we revisit the swirling squirmer problem considered by Binagia *et al.*[52] but in a shear-thinning, inelastic fluid to focus on the sole effect due to shear-thinning rheology. We use asymptotic analysis and numerical simulations to show explicitly that the addition of a swirling flow can either increase or decrease the speed of a squirmer in a shear-thinning fluid, depending on the rate of surface actuation relative to the critical shear rate of the shear-thinning fluid. We contrast the modifications on the translational and rotational swimming velocities by shear-thinning rheology alone with that due to fluid elasticity[52] to separate the effects due to these two features of non-Newtonian rheology. Taken together, the current work combines with previous studies to reveal qualitatively different features of a swirling squirmer in Newtonian, viscoelastic, and shear-thinning fluids.

This paper is organized as follows: We formulate the problem in Sec. II, introducing the squirmer model (Sec. II A), equations governing locomotion in a shear-thinning fluid (Sec. II B), and the non-dimensionalization used in this work (Sec. II C). In Sec. III, we first present the results from an asymptotic analysis at the small Carreau number limit (Sec. III A) before numerical results at a larger Carreau number (Sec. III B). Finally, we conclude this work in Sec. IV.

II. FORMULATION

A. The squirmer model

We consider the motion of a spherical squirmer of radius a (see setup and notations in Fig. 1). As a result of prescribed surface
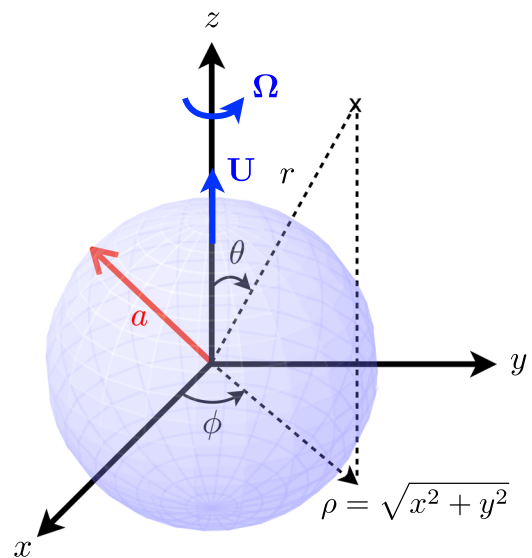
FIG. 1. The geometrical setup and notations of a swirling squirmer of radius a with tangential, axisymmetric squirming motion in both the polar (θ) and azimuthal (ϕ) directions. Here, $\rho = \sqrt{x^2 + y^2}$ denotes the perpendicular distance between a point to the z-axis. By symmetry, the translational ($\mathbf{U} = U\mathbf{e}_z$) and rotational ($\mathbf{\Omega} = \Omega\mathbf{e}_z$) swimming velocities are in the z-direction.

actuation $\mathbf{u}^S$, the squirmer swims at some translational ($\mathbf{U}$) and rotational ($\mathbf{\Omega}$) velocities. In the laboratory frame, the velocity at the surface of the squirmer is therefore given by

$$\mathbf{u}(r = a) = \mathbf{U} + \mathbf{\Omega} \times \mathbf{x}^S + \mathbf{u}^S, \qquad (1)$$

where $\mathbf{x}^S = a\mathbf{e}_r$ denotes the position vector of a point on the surface of the squirmer. A general representation of the tangential surface actuation of a steady, axisymmetric squirmer is given by[35,49]

$$\mathbf{u}^S(\theta) = \sum_{n=1}^{\infty} -\frac{2P_k^1(\cos\theta)}{k(k+1)} B_k \, \mathbf{e}_\theta + \sum_{n=1}^{\infty} -\frac{P_k^1(\cos\theta)}{a^{k+1}} C_k \, \mathbf{e}_\phi, \qquad (2)$$

where P_k^1 represents the associated Legendre function of the first kind, θ is the polar angle measured from the axis of symmetry, ϕ is the azimuthal angle, and the polar (B_k) and azimuthal (C_k) squirming modes can be related to Stokes flow singularity solutions.[49] Here, we follow the work of Binagia *et al.*[52] to consider a swirling squirmer consisting of the first two polar modes (B_1 and B_2) and the second azimuthal mode (C_2) as $\mathbf{u}^S = [B_1 \sin\theta + B_2 \sin(2\theta)/2] \mathbf{e}_\theta + 3C_2 \sin(2\theta)/2\mathbf{e}_\phi$. In a Newtonian fluid, only the B_1 mode (a source dipole) leads to a net swimming speed, $U_N = 2B_1/3$. The B_2 mode (a force dipole) can be used to represent a pusher ($\alpha = B_2/B_1 < 0$), which generates propulsion from its rear (e.g., the bacterium *Escherichia coli*), or a puller ($\alpha = B_2/B_1 > 0$), which generates propulsion from its front (e.g., the alga *Chlamydomonas*); the $\alpha = 0$ case is termed a neutral squirmer. Binagia *et al.*[52] added the C_2 mode (a rotlet dipole) to represent the effect due to a rotating flagellum and counter-rotating body of a swimming micro-organism.[53] We examine how such a biologically relevant swirling motion

couples with shear-thinning rheology to alter the swimming kinematics of a squirmer.

B. Governing equations

The incompressible flow around a squirmer is governed by the continuity equation and the Cauchy equation of motion in the absence of inertia,

$$\nabla \cdot \mathbf{u} = 0, \tag{3a}$$

$$\nabla \cdot \boldsymbol{\sigma} = \mathbf{0}, \tag{3b}$$

where the total stress $\boldsymbol{\sigma} = -p\mathbf{I} + \boldsymbol{\tau}$; here, $\mathbf{I}$ is the identity tensor, p and $\mathbf{u}$ represent the pressure and velocity fields, respectively, and $\boldsymbol{\tau}$ is the deviatoric stress tensor. To focus only on the shear-thinning effect, we consider a shear-thinning, inelastic fluid described by the Carreau constitutive law, $\boldsymbol{\tau} = \eta\dot{\boldsymbol{\gamma}}$, where the dynamic viscosity η is

$$\eta = \eta_\infty + (\eta_0 - \eta_\infty)\left(1 + \lambda_t^2|\dot{\boldsymbol{\gamma}}|^2\right)^{(n-1)/2} \tag{4}$$

and $\dot{\boldsymbol{\gamma}} = \nabla\mathbf{u} + (\nabla\mathbf{u})^{\mathrm{T}}$ is the strain rate tensor. Here, η_0 and η_∞ are the zero- and infinite-shear-rate viscosities, respectively. The power-law index n characterizes the degree of shear thinning ($n \leq 1$), and $1/\lambda_t$ represents a critical shear rate above which the shear-thinning effect becomes significant.

By symmetry, both the unknown translational and rotational velocities are oriented in the z-direction, $\mathbf{U} = U\mathbf{e}_z$ and $\boldsymbol{\Omega} = \Omega\mathbf{e}_z$, whose magnitudes can be determined by enforcing the force-free and torque-free conditions, respectively,

$$\int_S \boldsymbol{\sigma} \cdot \mathbf{n}\, \mathrm{d}S = \mathbf{0}, \tag{5a}$$

$$\int_S \mathbf{x}^S \times (\boldsymbol{\sigma} \cdot \mathbf{n})\, \mathrm{d}S = \mathbf{0}, \tag{5b}$$

where $\mathbf{n} = \mathbf{e}_r$ is the outward unit normal vector on the surface of the squirmer, S.

C. Non-dimensionalization

We scale lengths by the radius of the squirmer a, velocities by the first squirming mode B_1, strain rates by $\omega = B_1/a$, and stresses by $\eta_0\omega$. The constitutive equation therefore takes the dimensionless form

$$\boldsymbol{\tau}^* = \left[\beta + (1-\beta)\left(1 + Cu^2|\dot{\boldsymbol{\gamma}}^*|\right)^{(n-1)/2}\right]\dot{\boldsymbol{\gamma}}^*, \tag{6}$$

where $\beta = \eta_\infty/\eta_0$ is the viscosity ratio and $Cu = \lambda_t\omega$ is the Carreau number comparing the characteristics shear rate ω to the critical shear rate $1/\lambda_t$. Dimensionless variables are denoted with stars ($*$).

The dimensionless surface actuation of the swirling squirmer is given by

$$\mathbf{u}^{S*} = \sin\theta + \frac{\alpha}{2}\sin(2\theta)\,\mathbf{e}_\theta + \frac{3\zeta}{2}\sin(2\theta)\,\mathbf{e}_\phi, \tag{7}$$

where $\alpha = B_2/B_1$ represents the type of swimmer and $\zeta = C_2/(B_1a^3)$ measures the relative strength of the azimuthal flow to the polar

flow.[52] Hereafter, we drop the stars for simplicity and consider only dimensionless variables unless otherwise stated.

III. RESULTS AND DISCUSSION

A. Asymptotic analysis at small Carreau number

We use asymptotic analysis to reveal the first non-Newtonian correction to the swimming velocities in the limit of small Carreau number, $Cu^2 \ll 1$. We consider regular perturbation expansions for the variables in powers of Cu^2 as

$$\begin{aligned}
\{\mathbf{u}, p, \dot{\boldsymbol{\gamma}}, \boldsymbol{\tau}, \boldsymbol{\sigma}, \mathbf{U}, \boldsymbol{\Omega}\} &= \{\mathbf{u}_0, p_0, \dot{\boldsymbol{\gamma}}_0, \boldsymbol{\tau}_0, \boldsymbol{\sigma}_0, \mathbf{U}_0, \boldsymbol{\Omega}_0\} \\
&+ Cu^2\{\mathbf{u}_1, p_1, \dot{\boldsymbol{\gamma}}_1, \boldsymbol{\tau}_1, \boldsymbol{\sigma}_1, \mathbf{U}_1, \boldsymbol{\Omega}_1\} \\
&+ O(Cu^4).
\end{aligned} \tag{8}$$

1. Zeroth-order solution

The $O(Cu^0)$ solution corresponds to the motion in a Newtonian fluid, governed by the Stokes equation,

$$\nabla \cdot \mathbf{u}_0 = 0, \tag{9a}$$

$$\nabla \cdot \boldsymbol{\sigma}_0 = \mathbf{0}, \tag{9b}$$

where $\boldsymbol{\sigma}_0 = -p_0\mathbf{I} + \dot{\boldsymbol{\gamma}}_0$, with the boundary condition $\mathbf{u}_0(r=1) = \mathbf{U}_0 + \boldsymbol{\Omega}_0 \times \mathbf{x}^S + \mathbf{u}^S$, where $\mathbf{u}^S$ is given by Eq. (7). The zeroth-order solution, $\mathbf{u}_0 = u_0\mathbf{e}_r + v_0\mathbf{e}_\theta + w_0\mathbf{e}_\phi$ and p_0, is derived as

$$u_0 = \frac{U_0}{r^3}\cos\theta + \frac{\alpha}{4}\left(\frac{1}{r^4} - \frac{1}{r^2}\right)(1 + 3\cos 2\theta), \tag{10a}$$

$$v_0 = \frac{U_0}{2r^3}\sin\theta + \frac{\alpha}{2r^4}\sin 2\theta, \tag{10b}$$

$$w_0 = \frac{\Omega_0}{r^2}\sin\theta + \frac{3\zeta}{2r^3}\sin 2\theta, \tag{10c}$$

$$p_0 = -\frac{\alpha}{2r^3}(1 + 3\cos 2\theta). \tag{10d}$$

By enforcing the force-free and torque-free conditions at this order [Eqs. (5a) and (5b)], we recover the results in the Newtonian limit,[36,37,49]

$$U_0 = U_N = 2/3, \tag{11a}$$

$$\Omega_0 = 0. \tag{11b}$$

We note that adding the azimuthal flow in a Newtonian fluid does not generate any rotational velocity here.[49]

2. First-order solution

The $O(Cu^2)$ solution is governed by the continuity and momentum equations at this order,

$$\nabla \cdot \mathbf{u}_1 = 0, \tag{12a}$$

$$\nabla \cdot \boldsymbol{\sigma}_1 = \mathbf{0}, \tag{12b}$$

where $\boldsymbol{\sigma}_1 = -p_1\mathbf{I} + \dot{\boldsymbol{\gamma}}_1 + \mathbf{A}$ and

$$\mathbf{A} = \frac{(n-1)(1-\beta)}{2}|\dot{\boldsymbol{\gamma}}_0|^2\dot{\boldsymbol{\gamma}}_0. \tag{13}$$

The boundary condition at this order reads

$$\mathbf{u}_1(r=1) = \mathbf{U}_1 + \boldsymbol{\Omega}_1 \times \mathbf{x}^S. \tag{14}$$

To determine the leading-order correction to the translational ($\mathbf{U}_1$) and rotational ($\boldsymbol{\Omega}_1$) velocities, we exploit the reciprocal theorem to bypass detailed calculations of the flow at this order.[30,54–56] To apply the theorem, we consider an auxiliary flow problem for a body with identical geometry as our main problem (a sphere). The auxiliary flow ($\hat{\mathbf{u}}$) and stress ($\hat{\boldsymbol{\sigma}}$) fields satisfy the Stokes equation,

$$\nabla \cdot \hat{\mathbf{u}} = 0, \tag{15a}$$

$$\nabla \cdot \hat{\boldsymbol{\sigma}} = \mathbf{0}, \tag{15b}$$

where $\hat{\boldsymbol{\sigma}} = -\hat{p}\mathbf{I} + \hat{\boldsymbol{\tau}}$. All quantities in the auxiliary problem are denoted with hats. The reciprocal theorem then relates the force ($\hat{\mathbf{F}}$) and torque ($\hat{\mathbf{L}}$) on the body in the auxiliary problem to the first-order swimming kinematics as[55]

$$\hat{\mathbf{F}} \cdot \mathbf{U}_1 + \hat{\mathbf{L}} \cdot \boldsymbol{\Omega}_1 = \int_V \mathbf{A} : \nabla\hat{\mathbf{u}}\,\mathrm{d}V, \tag{16}$$

where the integral is over the entire fluid volume, V. We first determine $\mathbf{U}_1 = U_1\mathbf{e}_z$ by considering the Stokes flow due to a sphere translating at a unit speed in the z-direction as the auxiliary problem, $\hat{\mathbf{F}} = -6\pi\mathbf{e}_z$ and $\hat{\mathbf{L}} = \mathbf{0}$, leading to

$$U_1 = -\frac{1}{6\pi}\int_V \mathbf{A} : \nabla\hat{\mathbf{u}}\,\mathrm{d}V \tag{17}$$

$$= (1-\beta)\frac{(n-1)}{2}c_1(1 + c_2\alpha^2 + c_3\zeta^2), \tag{18}$$
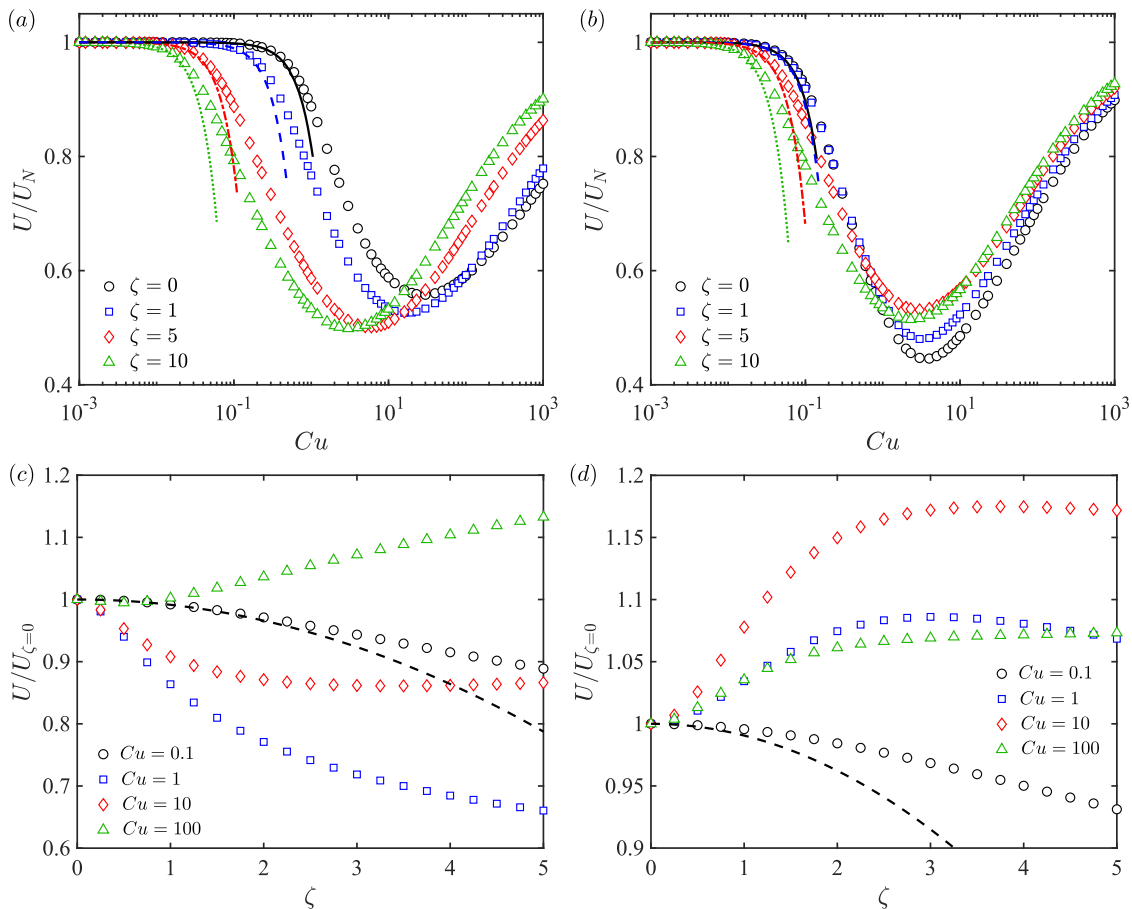
FIG. 2. Translational swimming velocity scaled by the Newtonian value, U/U_N, vs the Carreau number, Cu, for (a) a neutral squirmer ($\alpha = 0$) and (b) a pusher ($\alpha = -5$) for different strengths of the azimuthal mode, ζ. In (a) and (b), the numerical results (symbols) agree well with the corresponding asymptotic solution [Eq. (19)] for $\zeta = 0$ (black solid lines), $\zeta = 1$ (blue dashed lines), $\zeta = 5$ (red dotted-dashed lines), and $\zeta = 10$ (green dotted lines) at small Cu. The translational swimming speed relative to the case of no swirl, $U/U_{\zeta=0}$, as a function of the strength of the azimuthal mode, ζ, at different values of Cu for (c) a neutral squirmer and (d) a pusher. In (c) and (d), the black dashed lines represent the asymptotic solution based on Eq. (19). Results for pullers ($\alpha = 5$) are indistinguishable from those for pushers in (b) and (d) and, therefore, are not shown for simplicity. Here, $n = 0.25$ and $\beta = 0.01$.

where $c_1 = 64/195$, $c_2 = 1383/616$, and $c_3 = 369/77$. From Eq. (18), we see that the first shear-thinning correction $U_1 < 0$ as $n < 1$. The asymptotic result suggests that the azimuthal mode (ζ) further reduces the swimming speed at small Cu in a shear-thinning fluid, in contrast to the observation of enhanced speed in a viscoelastic fluid.[52] The speed modification U_1 is quadratic in ζ, implying that the sign of ζ does not affect the translational swimming velocity, as expected, by mirror symmetry. Combining Eqs. (9a) and (18), the asymptotic swimming speed including the first-order correction is

$$U \sim \frac{2}{3} + Cu^2 (1 - \beta) \frac{(n-1)}{2} c_1 (1 + c_2 \alpha^2 + c_3 \zeta^2). \quad (19)$$

The rotational velocity $\boldsymbol{\Omega}_1 = \Omega_1 \mathbf{e}_z$ can be similarly obtained with Eq. (16) by considering the Stokes flow of a sphere rotating at a unit speed in the z-direction as the auxiliary problem: $\hat{\mathbf{F}} = \mathbf{0}$ and $\hat{\mathbf{L}} = -8\pi \mathbf{e}_z$, resulting in

$$\Omega_1 = -\frac{1}{8\pi} \int_V \mathbf{A} : \nabla \hat{\mathbf{u}} \, dV \quad (20)$$

$$= -(1 - \beta) \frac{(n-1)}{2} c_4 \alpha \zeta, \quad (21)$$

where $c_4 = 2400/1001$. In contrast to zero rotation ($\Omega_0 = 0$) in a Newtonian fluid, Eq. (21) reveals that a swirling ($\zeta \neq 0$) pusher/puller ($\alpha \neq 0$) rotates in a shear-thinning fluid, while a swirling neutral squirmer does not. Moreover, a swirling pusher rotates in an opposite direction to that of a swirling puller. Results from the asymptotic analysis at small Cu here are shown in Figs. 2 and 3 and compared with numerical solutions of the full governing equations presented in Sec. III B. Similar to Eq. (19), we obtain the asymptotic rotational velocity as

$$\Omega \sim Cu^2 (1 - \beta) \frac{(n-1)}{2} c_4 \alpha \zeta. \quad (22)$$
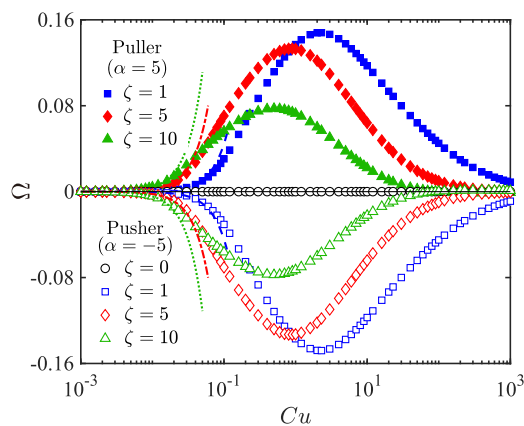
FIG. 3. Dimensionless rotational velocity, Ω, vs the Carreau number, Cu, for a pusher ($\alpha = -5$) and a puller ($\alpha = 5$) for different strengths of the azimuthal modes, ζ. The numerical results (symbols) agree well with the corresponding asymptotic [Eq. (22)] for $\zeta = 0$ (black solid lines), $\zeta = 1$ (blue dashed lines), $\zeta = 5$ (red dotted-dashed lines), and $\zeta = 10$ (green dotted lines) at small Cu. The rotational velocity of a neutral squirmer is negligibly small, consistent with the prediction by Eq. (22), and is therefore not shown. Here, $n = 0.25$ and $\beta = 0.01$.

In addition to the small Cu limit, weakly non-Newtonian behaviors also arise when the viscosity ratio β is close to unity. We can therefore conduct an asymptotic analysis in the limit $\varepsilon = 1 - \beta \ll 1$. We provide more details for this asymptotic analysis in the Appendix.

B. Numerical simulations at finite Carreau number

Next, we conduct numerical simulations to examine the behavior at larger values of Cu. We obtain the numerical solution of the continuity equation [Eq. (3a)] and the momentum equation [Eq. (3b)] with the Carreau constitutive model [Eq. (4)] based on a finite element method implemented in COMSOL. Because of its axisymmetry about the z-axis, the flow is solved on the ρz-plane of the cylindrical coordinate system (ρ, ϕ, z) (see Fig. 1). Note that the azimuthal flow u_ϕ does not depend on ϕ. Since flows at a low Reynolds number are expected to decay slowly, a large computational domain ($500 \times 500a^2$) is used to guarantee accuracy. The domain is discretized by ~30 000–50 000 Taylor–Hood ($P2 - P1$) triangular elements, with mesh refinement near the squirmer to properly capture the spatial variation of the viscosity. We perform the simulations in a reference frame moving with the squirmer. The force-free and torque-free conditions are implemented as global equations in COMSOL, which are solved together with the continuity and momentum equations; hence, the translational and rotational velocities are obtained simultaneously with the flow field. This approach is more efficient than the one used in our previous studies,[18,19,30] where we calculated the hydrodynamic forces on the squirmer using different inlet velocities and interpolated the one corresponding to zero force. The numerical implementation has been validated against analytical results in a Newtonian fluid[36,37,49] and shear-thinning fluids.[30,47] As a remark, we consider only positive values of ζ in this work because, by mirror symmetry, a sign reversal of ζ does not alter the translational swimming velocity[52] and only reverses the direction but not change the magnitude of the rotational velocity.

First, the numerical solutions of the non-Newtonian translational swimming velocities, scaled by the Newtonian value, U/U_N, are shown in Fig. 2 for a wide range of Cu. The asymptotic solution (lines) predicts well the numerical results (symbols) for various strengths of the azimuthal flow, ζ, when $Cu \ll 1$. For each value of ζ, the variation of the swimming speed is non-monotonic: the speed first decreases from the Newtonian value quadratically with increased Cu as predicted by the asymptotic solution (lines) based on Eq. (18). As Cu further increases, the speed reaches a minimum before approaching the Newtonian value again at a very large Cu, when the fluid viscosity becomes virtually uniform with the infinite-shear-rate value η_∞ at such high shear rates. In contrast to a swirling squirmer in a viscoelastic fluid, where faster than Newtonian swimming occurs;[52] here, a swirling neutral squirmer [Fig. 2(a)] and pusher/puller [Fig. 2(b)] always swim slower in a shear-thinning fluid ($U/U_N < 1$) for a wide range of Carreau numbers and strengths of azimuthal flow considered.

We note that although the shear-thinning effect does not increase the swimming speed compared to the Newtonian case, our numerical results reveal that in a shear-thinning fluid, the swirling motion can occasionally enhance the swimming speed of a squirmer,
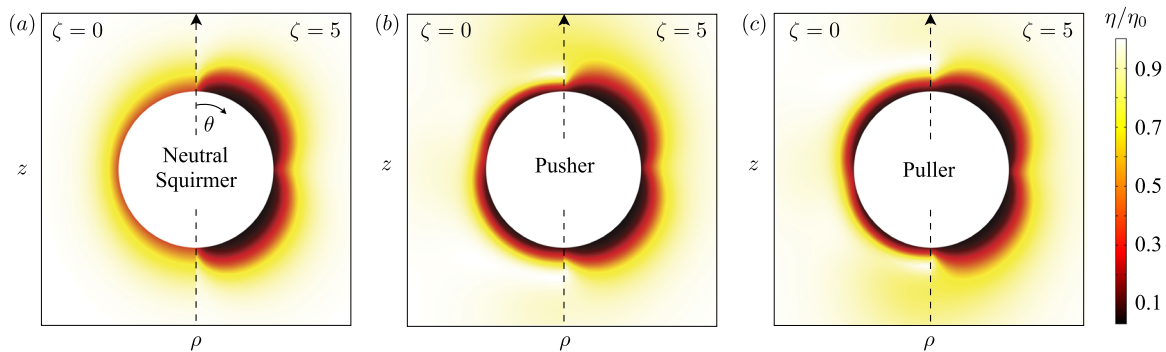
FIG. 4. Distribution of the viscosity scaled by the zero-shear-rate viscosity η/η_0 on the plane containing the axis of symmetry (i.e., the ρz-plane) for (a) a neutral squirmer ($\alpha = 0$), (b) a pusher ($\alpha = -5$), and (c) a puller ($\alpha = 5$). In (a)–(c), the left panel corresponds to a non-swirling squirmer and the right panel corresponds to a swirling counterpart with $\zeta = 5$. The color indicates the magnitude of η/η_0 and the vertical arrow indicates the swimming direction. Here, $n = 0.25$, $\beta = 0.01$, and $Cu = 1$.

depending on the Carreau number. We explore these behaviors in Figs. 2(c) and 2(d). At small Cu (e.g., $Cu = 0.1$), a stronger azimuthal mode (increasing ζ) monotonically reduces the swimming speed of a squirmer as predicted by the asymptotic analysis [Eq. (18); dashed black lines in Figs. 2(c) and 2(d)]. However, at larger values of Cu, more complex variations with ζ occur. At a sufficiently large Cu [e.g., $Cu = 100$ for a neutral squirmer in Fig. 2(c); green triangles], increasing the swirling strength enhances the swimming speed, $U/U_{\zeta=0} > 1$. The same trend is observed for a pusher/puller shown in Fig. 2(d), where a swirling squirmer swims faster than a non-swirling one when $Cu = 1$ or above. To conclude, the swirling motion coupled with the shear-thinning rheology can either decrease (at small Cu) or increase (at high Cu) the speed of a squirmer. Nevertheless, the resulting non-Newtonian swimming speed does not exceed the Newtonian counterpart for the wide range of Cu or ζ considered. These results therefore support the conclusion by Binagia *et al.*[52] that viscoelasticity is responsible for the enhanced locomotion of a swirling squirmer in a shear-thinning, viscoelastic fluid, compared with the case in a Newtonian fluid.

We next discuss the rotational velocity of a swirling squirmer in a shear-thinning fluid (Fig. 3). As shown in Eqs. (11a) and (11b), the swirling squirmer does not rotate in a Newtonian fluid. However, as shown in Fig. 3, the shear-thinning viscosity induces the rotation of a swirling pusher/puller as predicted asymptotically by Eq. (21) (lines) and numerically (symbols). For each value of ζ, the rotational velocity of a swirling pusher/puller increases quadratically with Cu in the small Cu regime and reaches a maximum value before decaying to zero at a very large Cu. The rotational velocities of a pusher and puller have the same magnitude but opposite direction as predicted by Eq. (21). A neutral, swirling squirmer however does not rotate in a shear-thinning fluid. We can better understand these results by examining the viscosity distribution around the squirmer in the plane containing the axis of symmetry (i.e., the ρz-plane) in Fig. 4. For a neutral squirmer, the magnitude of the surface velocity and, hence, the shear rate are symmetric about the equator ($\theta = \pi/2$). The viscosity distribution hence displays the same symmetry as shown in Fig. 4(a) when there is no swirl ($\zeta = 0$). Since the C_2 azimuthal flow is anti-symmetric (same magnitude but opposite sign) about the

equator, the modified hydrodynamic torque due to the shear-thinning effect on the northern hemisphere ($\theta \in [0, \pi/2]$) is the same as that on the southern hemisphere ($\theta \in [\pi/2, \pi]$). The squirmer is hence torque-free by symmetry and does not rotate even in the presence of the swirling motion and shear-thinning viscosity. On the other hand, the simultaneous presence of the B_1 and B_2 modes breaks the symmetry of the surface velocity and shear rate about the equator. The viscosity distribution is hence no longer symmetric about the equator for a pusher [Fig. 4(b)] and puller [Fig. 4(c)]. In the presence of the anti-symmetric C_2 azimuthal flow, the torques on the northern and southern hemispheres are modified differently by the shear-thinning viscosity. The imbalance in the torque therefore drives the rotation of the squirmer in order for it to remain torque-free. To illustrate this imbalance, we examine the hydrodynamic torque density about the z-axis, namely, $\ell_z(\theta) = \rho(\boldsymbol{\sigma} \cdot \mathbf{n}) \cdot \mathbf{e}_\phi$, as a function of θ, when the squirmer is not allowed
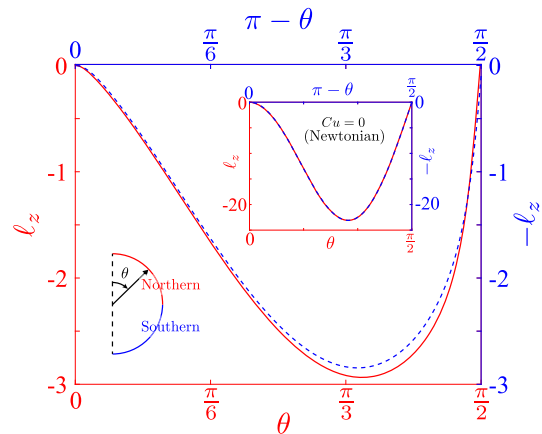
FIG. 5. Distribution of the torque density $\ell_z(\theta)$ on the northern hemisphere (red solid line and axes) and $-\ell_z(\pi - \theta)$ on the southern counterpart (blue dashed line and axes) for a non-rotating, swirling pusher ($\alpha = -5$ and $\zeta = 5$) shown in Fig. 4(b) ($n = 0.25$, $\beta = 0.01$, and $Cu = 1$). The inset depicts the corresponding Newtonian case ($Cu = 0$).

to rotate. The total torque acts only in the z-direction by axisymmetry and is given by integration, $L_z = 2\pi \int_0^\pi \ell_z \rho d\theta$. In Fig. 5, we contrast the torque density ℓ_z over the northern hemisphere (red solid line and axes) with that over the southern counterpart (blue dashed line and axes) in Newtonian (inset) and shearthinning fluids. In the Newtonian case ($Cu = 0$, inset), the symmetry in torque density about the equator leads to zero imbalanced torque and hence zero rotational velocity, as expected. In contrast, shear-thinning rheology breaks the symmetry of the torque density, resulting in a net torque imbalance that drives the rotation of the squirmer.

For sufficiently small Cu and ζ, the rotational velocity Ω increases monotonically with ζ in Fig. 3 as predicted by Eq. (22). However, note that the shear-thinning effect not only causes the imbalances in the torque but also reduces the magnitude of the torque simultaneously due to the decreased viscosity. Therefore, the overall magnitude of the imbalanced torque and

hence Ω could decrease with larger values of Cu and/or ζ, as shown in Fig. 3. Finally, at exceedingly large Cu, the viscosity approaches another Newtonian limit with an infinite-shearrate viscosity. The rotational velocity therefore decays to zero in this regime.

IV. CONCLUSION

The performance of a swimmer depends largely on its locomotory gaits and the properties of its surrounding fluid medium. In this work, we focus on the effects due to a biologically relevant azimuthal flow generated by a rotating flagellum and counterrotating body of a swimming bacterium via the squirmer model. While such a swirling motion has no effect on the swimming motion in a Newtonian fluid,[49] Binagia et al.[52] showed recently that it can couple with fluid elasticity to enhance the translational and
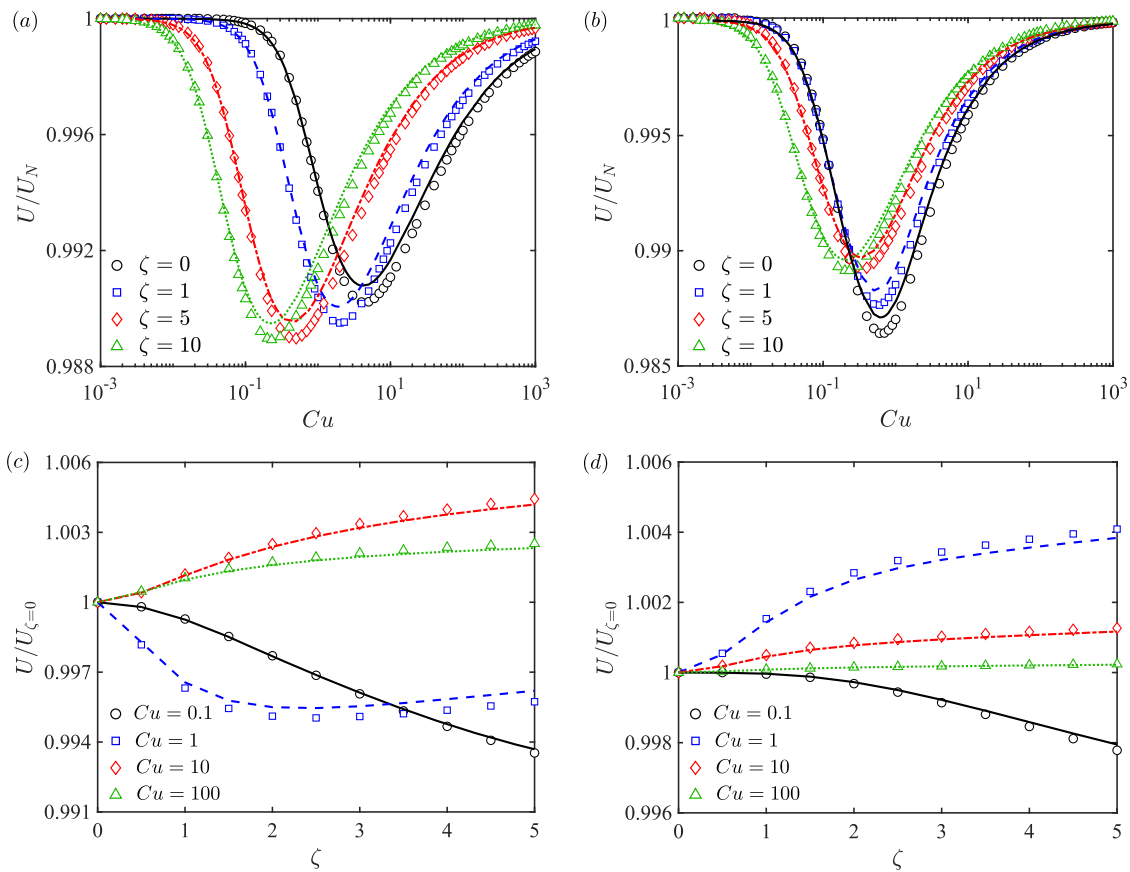
FIG. 6. Asymptotic (lines) and numerical (symbols) results in the small $\varepsilon = 1 - \beta$ regime. The translational swimming speed scaled by the Newtonian value, U/U_N, vs the Carreau number, Cu for (a) a neutral squirmer ($\alpha = 0$) and (b) a pusher ($\alpha = -5$). In (a) and (b), the numerical results (symbols) agree well with the corresponding asymptotic solutions for $\zeta = 0$ (black solid lines), $\zeta = 1$ (blue dashed lines), $\zeta = 5$ (red dotted-dashed lines), and $\zeta = 10$ (green dotted lines) when $\varepsilon = 0.1$. The translational swimming speed relative to the case of no swirl, $U/U_{\zeta=0}$, as a function of the strength of the azimuthal mode, ζ, for (c) a neutral squirmer ($\alpha = 0$) and (d) a pusher ($\alpha = -5$) at different values of Cu. In (c) and (d), the numerical results (symbols) agree well with the corresponding asymptotic solution for $Cu = 0.1$ (black solid lines), $Cu = 1$ (blue dashed lines), $Cu = 10$ (red dotted-dashed lines), and $Cu = 100$ (green dotted lines) for $\varepsilon = 0.1$. Results for pullers ($\alpha = 5$) are indistinguishable from that for pushers in (b) and (d) and are therefore not shown for simplicity. Here, $n = 0.25$.

rotational swimming velocities of the squirmer. Here, we examine the impacts of such a swirling flow on the locomotion of a squirmer in a fluid with shear-thinning viscosity, which is another ubiquitous non-Newtonian characteristic of biological fluids. Our asymptotic and numerical analyses show that shear-thinning rheology modifies the swimming kinematics of the squirmer in qualitatively different manners than fluid elasticity; while the swirling motion generally contributes to a decrease in the swimming speed of a squirmer at small Cu, it can also enhance the speed given a sufficiently large Cu. Despite any speed enhancement relative to a non-swirling squirmer, our results show that a swirling neutral squirmer, pusher, or puller always swim slower in a shear-thinning fluid than in a Newtonian fluid, in contrast to the case in a viscoelastic fluid.[52] In addition to translational swimming motion, we elucidate how the rotational motion of a swirling pusher or puller can emerge from the coupling of the swirling flow and shear-thinning viscosity. Results from this note and previous studies, taken together, demonstrate how the same locomotory gaits can lead to vastly different swimming behaviors depending on the fluid rheology.

AUTHORS' CONTRIBUTIONS

H.N. and K.Z. contributed equally to this work.

APPENDIX: ASYMPTOTIC ANALYSIS AT SMALL $\varepsilon = 1 - \beta$

In addition to the small Cu limit, we can also conduct an asymptotic analysis in the small $\varepsilon = 1 - \beta \ll 1$ limit,

$$\{\mathbf{u}, p, \dot{\gamma}, \boldsymbol{\tau}, \boldsymbol{\sigma}, \mathbf{U}, \boldsymbol{\Omega}\} = \{\mathbf{u}_0, p_0, \dot{\gamma}_0, \boldsymbol{\tau}_0, \boldsymbol{\sigma}_0, \mathbf{U}_0, \boldsymbol{\Omega}_0\}$$
$$+ \varepsilon\{\mathbf{u}_1, p_1, \dot{\gamma}_1, \boldsymbol{\tau}_1, \boldsymbol{\sigma}_1, \mathbf{U}_1, \boldsymbol{\Omega}_1\} + O(\varepsilon^2). \quad (A1)$$

The solution procedure is similar to that in Sec. III A, so we only outline the main steps.

The zeroth-order solution corresponds to the Newtonian flow given by Eqs. (10a)–(10d). The fist-order solution is governed by equations of the same form as Eqs. (12a) and (12b) but with a different tensor $\mathbf{A}$ than Eq. (13),

$$\mathbf{A} = \left[-1 + \left(1 + Cu^2 |\dot{\gamma}_0|^2\right)^{(n-1)/2}\right]\dot{\gamma}_0. \quad (A2)$$

The first-order swimming kinematics can again be determined with the reciprocal theorem [Eq. (16)] to arrive at the same integral expressions for the translational [Eq. (17)] and rotational [Eq. (20)] velocities. By evaluating the integrals by quadrature, we obtain the asymptotic results (lines) shown in Fig. 6, which agree well with full

numerical simulations of the governing equations for $\varepsilon = 0.1$. Similar qualitative features are observed here as those described in the main text.

REFERENCES

[1] L. J. Fauci and R. Dillon, "Biofluidmechanics of reproduction," Annu. Rev. Fluid Mech. **38**, 371–394 (2006).

[2] E. Lauga and T. R. Powers, "The hydrodynamics of swimming microorganisms," Rep. Prog. Phys. **72**, 096601 (2009).

[3] J. M. Yeomans, D. O. Pushkin, and H. Shum, "An introduction to the hydrodynamics of swimming microorganisms," Eur. Phys. J. Spec. Top. **223**, 1771–1785 (2014).

[4] A. Zöttl and H. Stark, "Emergent behavior in active colloids," J. Phys.: Condens. Matter **28**, 253001 (2016).

[5] J. Zhang, E. Luijten, B. A. Grzybowski, and S. Granick, "Active colloids with collective mobility status and research opportunities," Chem. Soc. Rev. **46**, 5551–5569 (2017).

[6] W. Wang, X. Lv, J. L. Moran, S. Duan, and C. Zhou, "A practical guide to active colloids: Choosing synthetic model systems for soft matter physics research," Soft Matter **16**, 3846–3868 (2020).

[7] B. J. Nelson, I. K. Kaliakatsos, and J. J. Abbott, "Microrobots for minimally invasive medicine," Annu. Rev. Biomed. Eng. **12**, 55–85 (2010).

[8] S. Sengupta, M. E. Ibele, and A. Sen, "Fantastic voyage: Designing self-powered nanorobots," Angew. Chem. Int. Ed. **51**, 8434–8445 (2012).

[9] C. Hu, S. Pané, and B. J. Nelson, "Soft micro- and nanorobotics," Annu. Rev. Control Robot. Autonom. Syst. **1**, 53–75 (2018).

[10] G. J. Elfring and E. Lauga, "Theory of locomotion through complex fluids," in *Complex Fluids in Biological Systems*, edited by S. E. Spagnolie (Springer, New York, 2015), pp. 283–317.

[11] J. Sznitman and P. E. Arratia, "Locomotion through complex fluids: An experimental view," in *Complex Fluids in Biological Systems*, edited by S. E. Spagnolie (Springer, New York, 2015), pp. 245–281.

[12] Z. Wu, Y. Chen, D. Mukasa, O. S. Pak, and W. Gao, "Medical micro/nanorobots in complex media," Chem. Soc. Rev. (published online 2020).

[13] E. Lauga, "Propulsion in a viscoelastic fluid," Phys. Fluids **19**, 083104 (2007).

[14] H. C. Fu, C. W. Wolgemuth, and T. R. Powers, "Swimming speeds of filaments in nonlinearly viscoelastic fluids," Phys. Fluids **21**, 033102 (2009).

[15] J. Teran, L. Fauci, and M. Shelley, "Viscoelastic fluid response can increase the speed and efficiency of a free swimmer," Phys. Rev. Lett. **104**, 038101 (2010).

[16] X. N. Shen and P. E. Arratia, "Undulatory swimming in viscoelastic fluids," Phys. Rev. Lett. **106**, 208101 (2011).

[17] B. Liu, T. R. Powers, and K. S. Breuer, "Force-free swimming of a model helical flagellum in viscoelastic fluids," Proc. Natl. Acad. Sci. U. S. A. **108**, 19516–19520 (2011).

[18] L. Zhu, M. Do-Quang, E. Lauga, and L. Brandt, "Locomotion by tangential deformation in a polymeric fluid," Phys. Rev. E **83**, 011901 (2011).

[19] L. Zhu, E. Lauga, and L. Brandt, "Self-propulsion in viscoelastic fluids: Pushers vs pullers," Phys. Fluids **24**, 051902 (2012).

[20] O. S. Pak, L. Zhu, L. Brandt, and E. Lauga, "Micropropulsion and microrheology in complex fluids via symmetry breaking," Phys. Fluids **24**, 103102 (2012).

[21] S. E. Spagnolie, B. Liu, and T. R. Powers, "Locomotion of helical bodies in viscoelastic fluids: Enhanced swimming at large helical amplitudes," Phys. Rev. Lett. **111**, 068101 (2013).

[22] B. Thomases and R. D. Guy, "Mechanisms of elastic enhancement and hindrance for finite-length undulatory swimmers in viscoelastic fluids," Phys. Rev. Lett. **113**, 098102 (2014).

[23]B. Qin, A. Gopinath, J. Yang, J. P. Gollub, and P. E. Arratia, "Flagellar kinematics and swimming of algal cells in viscoelastic fluids," Sci. Rep. **5**, 9190 (2015).

[24]G. Li, G. H. McKinley, and A. M. Ardekani, "Dynamics of particle migration in channel flow of viscoelastic fluids," J. Fluid Mech. **785**, 486–505 (2015).

[25]C.-K. Tung, C. Lin, B. Harvey, A. G. Fiore, F. Ardon, M. Wu, and S. S. Suarez, "Fluid viscoelasticity promotes collective swimming of sperm," Sci. Rep. **7**, 3152 (2017).

[26]S. Sahoo, S. P. Singh, and S. Thakur, "Enhanced self-propulsion of a sphere-dimer in viscoelastic fluid," Soft Matter **15**, 2170–2177 (2019).

[27]T. D. Montenegro-Johnson, D. J. Smith, and D. Loghin, "Physics of rheologically enhanced propulsion: Different strokes in generalized Stokes," Phys. Fluids **25**, 081903 (2013).

[28]J. R. Vélez-Cordero and E. Lauga, "Waving transport and propulsion in a generalized Newtonian fluid," J. Non-Newtonian Fluid Mech. **199**, 37–50 (2013).

[29]G. Li and A. M. Ardekani, "Undulatory swimming in non-Newtonian fluids," J. Fluid Mech. **784**, R4 (2015).

[30]C. Datt, L. Zhu, G. J. Elfring, and O. S. Pak, "Squirming through shear-thinning fluids," J. Fluid Mech. **784**, R1 (2015).

[31]D. A. Gagnon, N. C. Keim, and P. E. Arratia, "Undulatory swimming in shear-thinning fluids: Experiments with *Caenorhabditis elegans*," J. Fluid Mech. **758**, R3 (2014).

[32]D. A. Gagnon and P. E. Arratia, "The cost of swimming in generalized Newtonian fluids: Experiments with *C. elegans*," J. Fluid Mech. **800**, 753–765 (2016).

[33]T. D. Montenegro-Johnson, "Fake μs: A cautionary tail of shear-thinning locomotion," Phys. Rev. Fluids **2**, 081101 (2017).

[34]S. Gómez, F. A. Godínez, E. Lauga, and R. Zenit, "Helical propulsion in shear-thinning fluids," J. Fluid Mech. **812**, R3 (2017).

[35]T. J. Pedley, "Spherical squirmers: Models for swimming micro-organisms," IMA J. Appl. Math. **81**, 488 (2016).

[36]M. J. Lighthill, "On the squirming motion of nearly spherical deformable bodies through liquids at very small Reynolds numbers," Commun. Pure Appl. Math. **5**, 109–118 (1952).

[37]J. R. Blake, "A spherical envelope approach to ciliary propulsion," J. Fluid Mech. **46**, 199 (1971).

[38]K. Drescher, R. E. Goldstein, and I. Tuval, "Fidelity of adaptive phototaxis," Proc. Natl. Acad. Sci. U. S. A. **107**, 11171–11176 (2010).

[39]T. Ishikawa, M. P. Simmonds, and T. J. Pedley, "Hydrodynamic interaction of two swimming model micro-organisms," J. Fluid Mech. **568**, 119–160 (2006).

[40]T. Ishikawa and T. J. Pedley, "Coherent structures in monolayers of swimming particles," Phys. Rev. Lett. **100**, 088103 (2008).

[41]G.-J. Li, A. Karimi, and A. M. Ardekani, "Effect of solid boundaries on swimming dynamics of microorganisms in a viscoelastic fluid," Rheol. Acta **53**, 911–926 (2014).

[42]S. Yazdi, A. M. Ardekani, and A. Borhan, "Locomotion of microorganisms near a no-slip boundary in a viscoelastic fluid," Phys. Rev. E **90**, 043002 (2014).

[43]M. De Corato, F. Greco, and P. L. Maffettone, "Locomotion of a microorganism in weakly viscoelastic liquids," Phys. Rev. E **92**, 053008 (2015).

[44]H. Nganguia, K. Pietrzyk, and O. S. Pak, "Swimming efficiency in a shear-thinning fluid," Phys. Rev. E **96**, 062606 (2017).

[45]C. Datt, G. Natale, S. G. Hatzikiriakos, and G. J. Elfring, "An active particle in a complex fluid," J. Fluid Mech. **823**, 675–688 (2017).

[46]K. Qi, E. Westphal, G. Gompper, and R. G. Winkler, "Enhanced rotational motion of spherical squirmer in polymer solutions," Phys. Rev. Lett. **124**, 068001 (2020).

[47]K. Pietrzyk, H. Nganguia, C. Datt, L. Zhu, G. J. Elfring, and O. S. Pak, "Flow around a squirmer in a shear-thinning fluid," J. Non-Newtonian Fluid Mech. **268**, 101–110 (2019).

[48]S. Ghose and R. Adhikari, "Irreducible representations of oscillatory and swirling flows in active soft matter," Phys. Rev. Lett. **112**, 118102 (2014).

[49]O. S. Pak and E. Lauga, "Generalized squirming motion of a sphere," J. Eng. Math. **88**, 1–28 (2014).

[50]B. U. Felderhof and R. B. Jones, "Stokesian swimming of a sphere at low Reynolds number by helical surface distortion," Phys. Fluids **28**, 073601 (2016).

[51]T. J. Pedley, D. R. Brumley, and R. E. Goldstein, "Squirmers with swirl: A model for volvox swimming," J. Fluid Mech. **798**, 165–186 (2016).

[52]J. P. Binagia, A. Phoa, K. D. Housiadas, and E. S. G. Shaqfeh, "Swimming with swirl in a viscoelastic fluid," J. Fluid Mech. **900**, A4 (2020).

[53]A. Chwang and T. Y. Wu, "A note on the helical movement of micro-organisms," Proc. R. Soc. London, Ser. B **178**, 327–346 (1971).

[54]H. A. Stone and A. D. T. Samuel, "Propulsion of microorganisms by surface distortions," Phys. Rev. Lett. **77**, 4102 (1996).

[55]E. Lauga, "Locomotion in complex fluids: Integral theorems," Phys. Fluids **26**, 081902 (2014).

[56]H. Masoud and H. A. Stone, "The reciprocal theorem in fluid dynamics and transport phenomena," J. Fluid Mech. **879**, P1 (2019).